Orthogonal Time Frequency Space (OTFS) Modulation

Tutorial at ICC2019, Shanghai, May 24th, 2019

Yi Hong[†]**, Emanuele Viterbo**[†] **A. Chockalingam,**[‡]

† Department of Electrical and Computer Systems Engineering
Monash University, Clayton, Australia

‡ Department of Electrical and Communications Engineering
Indian Institute of Science, Bangalore, India

Special thanks to

P. Raviteja, Tharaj Thaj, Khoa T.Phan, M.K. Ramachandran

Overview I

1. Introduction
   - Evolution of wireless
   - High-Doppler wireless channels
   - Conventional modulation schemes (e.g., OFDM)
   - Effect of high Dopplers in conventional modulation
2. Wireless channel representation
   - Time–frequency representation
   - Time–delay representation
   - Delay–Doppler representation
3. OTFS modulation
   - Signaling in the delay–Doppler domain
   - Compatibility with OFDM architecture

Overview II

4. OTFS Input-Output Relation in Matrix Form
5. OTFS Signal Detection
   - Vectorized formulation of the input-output relation
   - Message passing based detection
   - Other detectors
6. MIMO/multiuser MIMO OTFS
7. OTFS channel estimation
   - Channel estimation in delay-Doppler domain
   - Multiuser OTFS
8. OTFS applications
   - OTFS radar
   - SDR implementation of OTFS
   - OTFS with static multipath channels

Link to download Matlab code:

`https://ecse.monash.edu/staff/eviterbo/OTFS-VTC18/OTFS_sample_code.zip`

Introduction

Evolution of wireless

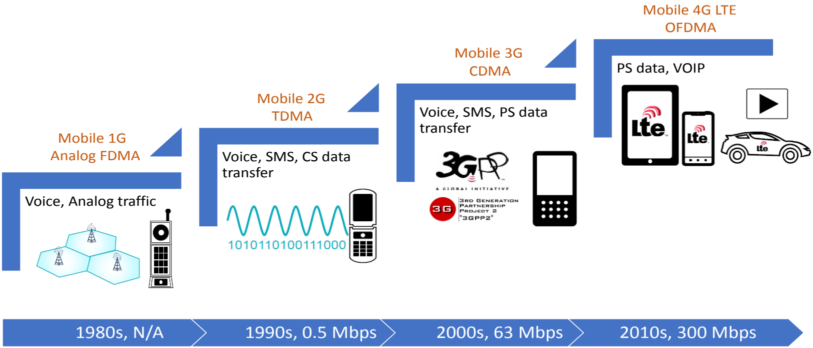

- Waveform design is the major change between the generations

High-Doppler wireless channels

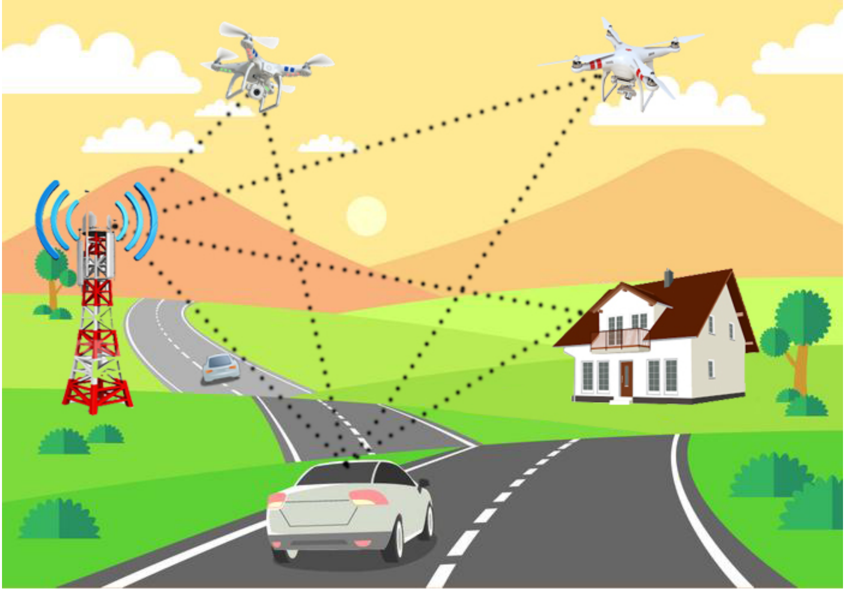

Wireless Channels - delay spread

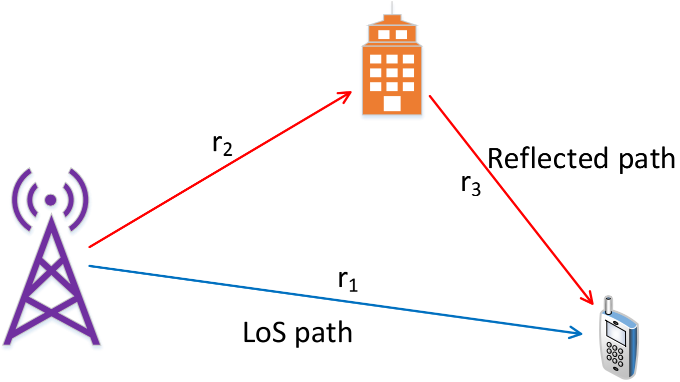

- Delay of LoS path: $\tau_1 = r_1/c$
- Delay of reflected path: $\tau_2 = (r_2 + r_3)/c$
- Delay spread: $\tau_2 - \tau_1$

Wireless Channels - Doppler spread

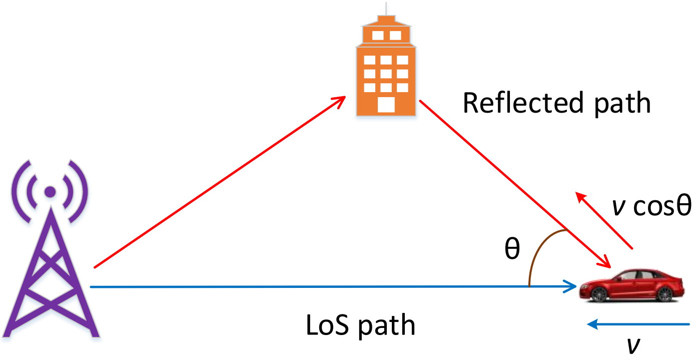

- Doppler frequency of LoS path: $\nu_1 = f_c \frac{v}{c}$
- Doppler frequency of reflected path: $\nu_2 = f_c \frac{v \cos\theta}{c}$
- Doppler spread: $\nu_2 - \nu_1$

Typical delay and Doppler spreads

Delay spread ($c = 3 \cdot 10^8$m/s)

$\Delta r_{\max}$	Indoor (3m)	Outdoor (3km)
$\tau_{\max}$	10ns	10μs

Doppler spread

$\nu_{\max}$	$f_c = 2$GHz	$f_c = 60$GHz
$v = 1.5$m/s $= 5.5$km/h	10Hz	300Hz
$v = 3$m/s $= 11$km/h	20Hz	600Hz
$v = 30$m/s $= 110$km/h	200Hz	6KHz
$v = 150$m/s $= 550$km/h	1KHz	30KHz

Conventional modulation scheme – OFDM

- OFDM - Orthogonal Frequency Division Multiplexing

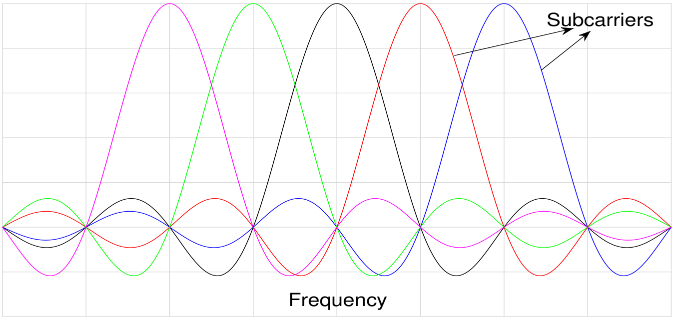

- OFDM divides the frequency selective channel into multiple parallel sub-channels

OFDM system model

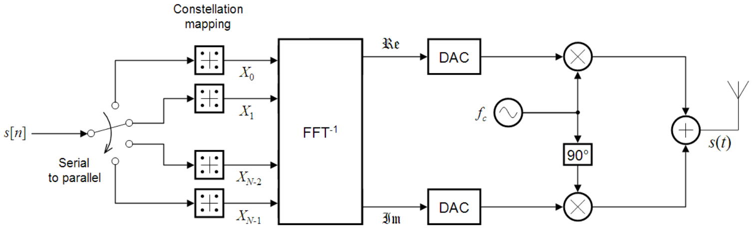

Figure: OFDM Tx

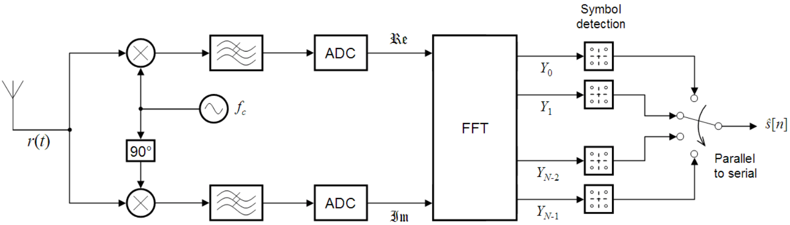

Figure: OFDM Rx

(*) From Wikipedia, the free encyclopedia

OFDM system model

- Received signal – channel is constant over OFDM symbol (no Doppler)
  $h_0, h_1, \cdots, h_{P-1}$ – Path gains over P taps

$$
\mathbf{r} = \underbrace{\begin{bmatrix}
h_0 & 0 & \cdots & 0 & h_{P-1} & h_{P-2} & \cdots & h_1 \\
h_1 & h_0 & \cdots & 0 & 0 & h_{P-1} & \cdots & h_2 \\
\vdots & \ddots & \ddots & \ddots & \ddots & \ddots & \ddots & \vdots \\
\vdots & \ddots & \ddots & \ddots & \ddots & \ddots & \ddots & h_{P-1} \\
h_{P-1} & \ddots & \ddots & \ddots & \ddots & \ddots & \ddots & \vdots \\
\vdots & \ddots & \ddots & \ddots & \ddots & \ddots & \ddots & \vdots \\
\vdots & \ddots & \ddots & \ddots & \ddots & \ddots & \ddots & \vdots \\
0 & 0 & \cdots & h_{P-1} & h_{P-2} & \cdots & h_1 & h_0
\end{bmatrix}}_{\text{Circulant matrix } (\mathbf{H})} \mathbf{s}
$$

OFDM system model

- At the receiver we have

$$\mathbf{r} = \mathbf{F}^H \mathbf{D} \mathbf{F} \mathbf{s} = \sum_{i=0}^{P-1} h_i \mathbf{\Pi}^i \mathbf{s}$$

where $\mathbf{\Pi}$ is the permutation matrix $\begin{pmatrix} 0 & \cdots & 0 & 1 \\ 1 & \ddots & 0 & 0 \\ \vdots & \ddots & \ddots & \vdots \\ 0 & \cdots & 1 & 0 \end{pmatrix}$

(notation used later as alternative representation of the channel)

- At the receiver we have

$$\mathbf{y} = \mathbf{F}\mathbf{r} = \underbrace{\mathbf{D}}_{\text{Diagonal matrix}} \mathbf{x}$$

- OFDM Pros
  - Simple detection (one tap equalizer)
  - Efficiently combat the multi-path effects

Effect of high multiple Dopplers in OFDM

- **H** matrix lost the circulant structure – decomposition becomes erroneous
- Introduces inter carrier interference (ICI)

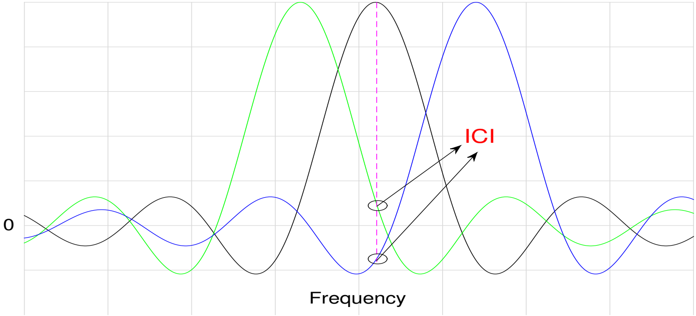

- OFDM Cons
  - multiple Dopplers are difficult to equalize
  - Sub-channel gains are not equal and lowest gain decides the performance

Effect of high Dopplers in OFDM

- Orthogonal Time Frequency Space Modulation (OTFS)$^{(*)}$
  - Solves the two cons of OFDM
  - Works in Delay–Doppler domain rather than Time–Frequency domain

(*) R. Hadani, S. Rakib, M. Tsatsanis, A. Monk, A. J. Goldsmith, A. F. Molisch, and R. Calderbank, "Orthogonal time frequency space modulation," in *Proc. IEEE WCNC*, San Francisco, CA, USA, March 2017.

Wireless channel representation

Wireless channel representation

- Different representations of linear time variant (LTV) wireless channels

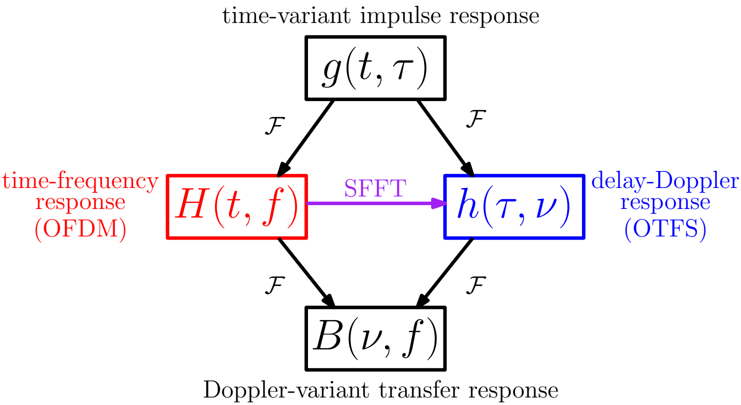

Wireless channel representation

- The received signal in linear time variant channel (LTV)

$$r(t) = \int \underbrace{g(t,\tau)}_{\text{time-variant impulse response}} s(t-\tau)d\tau \rightarrow \text{generalization of LTI}$$

$$= \int\int \underbrace{h(\tau,\nu)}_{\text{Delay–Doppler spreading function}} s(t-\tau)e^{j2\pi\nu t}d\tau d\nu \rightarrow \text{Delay–Doppler Channel}$$

$$= \int \underbrace{H(t,f)}_{\text{time-frequency response}} S(f)e^{j2\pi ft}df \rightarrow \text{Time–Frequency Channel}$$

- Relation between $h(\tau,\nu)$ and $H(t,f)$

$$\left.\begin{aligned} h(\tau,\nu) &= \int\int H(t,f)e^{-j2\pi(\nu t - f\tau)}dtdf \\ H(t,f) &= \int\int h(\tau,\nu)e^{j2\pi(\nu t - f\tau)}d\tau d\nu \end{aligned}\right\} \text{Pair of 2D symplectic FT}$$

Wireless channel representation

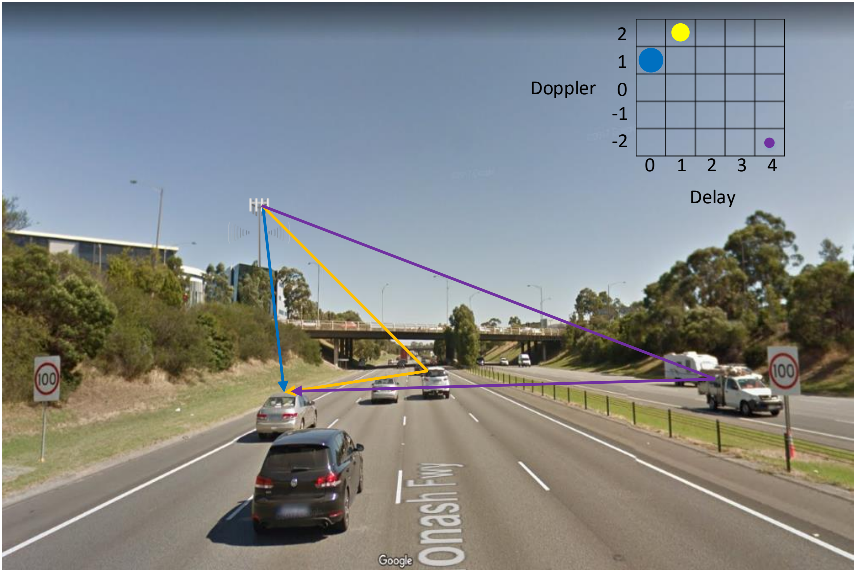

Wireless channel representation

Time-variant impulse response $g(t, \tau)$

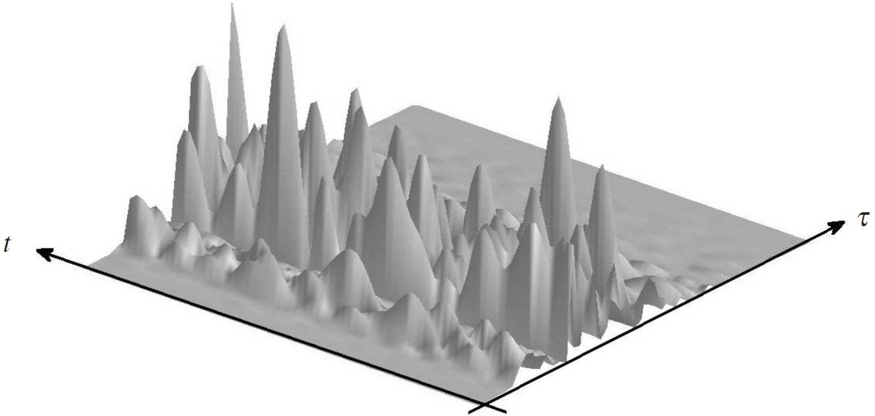

* G. Matz and F. Hlawatsch, *Chapter 1, Wireless Communications Over Rapidly Time-Varying Channels.* New York, NY, USA: Academic, 2011

Time-frequency and delay-Doppler responses

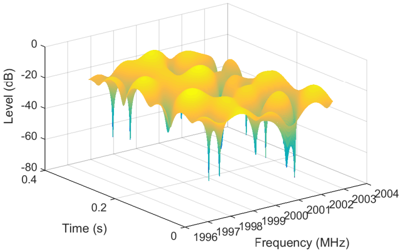

SFFT →

← ISFFT

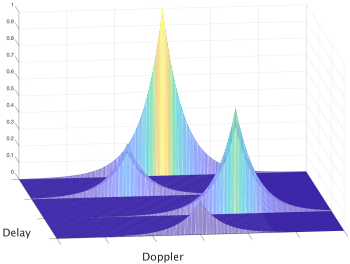

Channel in Time–frequency $H(t, f)$ and delay–Doppler $h(\tau, \nu)$

Time–Frequency and delay–Doppler grids

- Assume $\Delta f = 1/T$

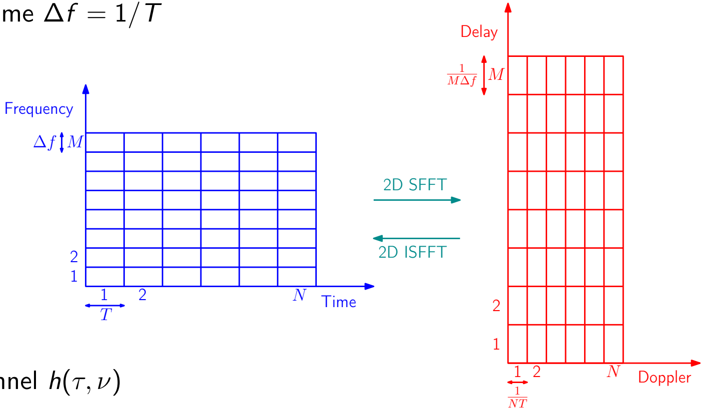

- Channel $h(\tau, \nu)$

$$h(\tau, \nu) = \sum_{i=1}^{P} h_i \delta(\tau - \tau_i)\delta(\nu - \nu_i)$$

- Assume $\tau_i = l_{\tau_i}\left(\frac{1}{M\Delta f}\right)$ and $\nu_i = k_{\nu_i}\left(\frac{1}{NT}\right)$

OTFS Parameters

Subcarrier spacing (Δf)	M	Bandwidth ($W = M\Delta f$)	Symbol duration ($T_s = 1/W$)	delay spread	$l_{\tau_{\max}}$
15 KHz	1024	**15 MHz**	0.067 μs	4.7 μs	71 ($\approx$ 7%)

Carrier frequency (f_c)	N	Latency ($NMT_s = NT$)	Doppler resolution ($1/NT$)	UE speed (v)	Doppler frequency ($f_d = f_c \frac{v}{c}$)	$k_{\nu_{\max}}$
4 GHz	128	**8.75 ms**	114 Hz	30 Kmph	111 Hz	1 ($\approx$ 1.5%)
				120 Kmph	444 Hz	4 ($\approx$ 6%)
				500 Kmph	1850 Hz	16($\approx$ 25%)

OTFS modulation

OTFS modulation

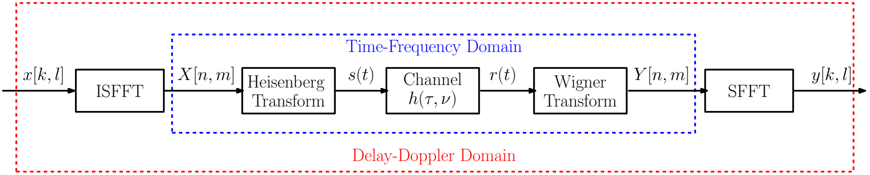

Figure: OTFS mod/demod

- Time–frequency domain is similar to an OFDM system with N symbols in a frame (Pulse-Shaped OFDM)

Time–frequency domain

- Modulator – Heisenberg transform

$$s(t) = \sum_{n=0}^{N-1} \sum_{m=0}^{M-1} X[n,m] g_{\text{tx}}(t - nT) e^{j2\pi m \Delta f (t - nT)}$$

- Simplifies to IFFT in the case of $N = 1$ and rectangular g_{tx}
- Channel

$$r(t) = \int H(t,f) S(f) e^{j2\pi f t} df$$

- Matched filter – Wigner transform

$$Y(t,f) = A_{g_{\text{rx}},r}(t,f) \triangleq \int g_{\text{rx}}^*(t' - t) r(t') e^{-j2\pi f (t' - t)} dt'$$

$$Y[n,m] = Y(t,f)|_{t=nT, f=m\Delta f}$$

- Simplifies to FFT in the case of $N = 1$ and rectangular g_{rx}

Time–frequency domain – ideal pulses

- If g_{tx} and g_{rx} are perfectly localized in time and frequency then they satisfy the bi-orthogonality condition and

$$Y[n,m] = H[n,m]X[n,m]$$

where

$$H[n,m] = \int\int h(\tau,\nu)e^{j2\pi\nu nT}e^{-j2\pi m\Delta f\tau}d\tau d\nu$$

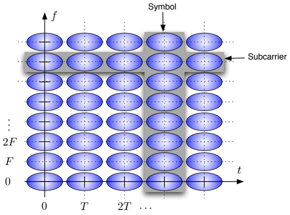

Figure: Time–frequency domain

---

* F. Hlawatsch and G. Matz, Eds., *Chapter 2, Wireless Communications Over Rapidly Time-Varying Channels.* New York, NY, USA: Academic, 2011 (PS-OFDM)

Signaling in the delay–Doppler domain

- Time–frequency input-output relation

$$Y[n, m] = H[n, m]X[n, m]$$

where

$$H[n, m] = \sum_k \sum_l h[k, l]\, e^{j2\pi\left(\frac{nk}{N} - \frac{ml}{M}\right)}$$

- ISFFT

$$X[n, m] = \frac{1}{\sqrt{NM}} \sum_{k=0}^{N-1} \sum_{l=0}^{M-1} x[k, l] e^{j2\pi\left(\frac{nk}{N} - \frac{ml}{M}\right)}$$

- SFFT

$$y[k, l] = \frac{1}{\sqrt{NM}} \sum_{n=0}^{N-1} \sum_{m=0}^{M-1} Y[n, m] e^{-j2\pi\left(\frac{nk}{N} - \frac{ml}{M}\right)}$$

Delay–Doppler domain input-output relation

- Received signal in delay–Doppler domain

$$y[k,l] = \sum_{i=1}^{P} h_i x[[k - k_{\nu_i}]_N, [l - l_{\tau_i}]]_M$$
$$= h[k,l] \circledast x[k,l] \qquad \text{(2D Circular Convolution)}$$

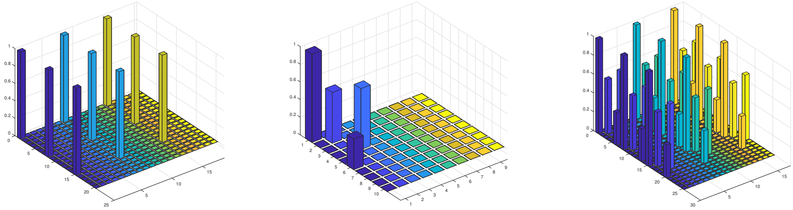

(a) Input signal, $x[k,l]$ (b) Channel, $h[k,l]$ (c) Output signal, $y[k,l]$

Figure: OTFS signals

Fractional doppler effect

- Actual Doppler may not be perfectly aligned with the grid

$$\nu_i = (k_{\nu_i} + \kappa_{\nu_i}) \left(\frac{1}{NT} \right), k_{\nu_i} \in \mathbb{Z}, -1/2 < \kappa_{\nu_i} < 1/2$$

- Induces interference from the neighbor points of k_{ν_i} in the Doppler grid due to non-orthogonality in channel relation – Inter Doppler Interference (IDI)
- Received signal equation becomes

$$y(k,l) = \sum_{i=1}^{P} \sum_{q=-N_i}^{N_i} h_i \left(\frac{e^{j2\pi(-q-\kappa_{\nu_i})} - 1}{Ne^{j\frac{2\pi}{N}(-q-\kappa_{\nu_i})} - N} \right) x\left[[k - k_{\nu_i} + q]_N, [l - l_{\tau_i}]_M\right]$$

Compatibility with OFDM architecture

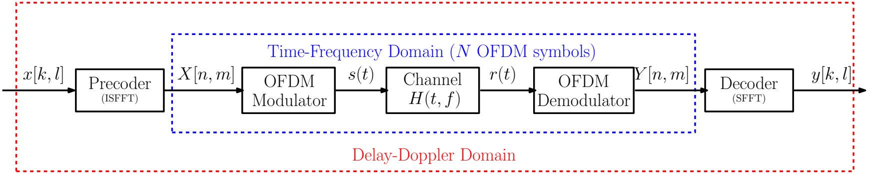

Figure: OTFS mod/demod

- OTFS is compatible with LTE system
- OTFS can be easily implemented by applying a precoding and decoding blocks on N consecutive OFDM symbols

OTFS with rectangular pulses – time–frequency domain

- Assume g_{tx} and g_{rx} to be rectangular pulses (same as OFDM) – don't follow bi-orthogonality condition

- Time–frequency input-output relation

$$Y[n, m] = H[n, m]X[n, m] + \text{ICI} + \text{ISI}$$

- ICI – loss of orthogonality in frequency domain due to Dopplers

- ISI – loss of orthogonality in time domain due to delays

(*) P. Raviteja, K. T. Phan, Y. Hong, and E. Viterbo, "Interference cancellation and iterative detection for orthogonal time frequency space modulation," *IEEE Trans. Wireless Commun.*, vol. 17, no. 10, pp. 6501-6515, Oct. 2018. Available on: https://arxiv.org/abs/1802.05242

OTFS Input-Output Relation in Matrix Form

OTFS: matrix representation

- Transmit signal at time–frequency domain: ISFFT+Heisenberg+pulse shaping on delay–Doppler

$$\mathbf{S} = \mathbf{G}_{\mathrm{tx}}\mathbf{F}_M^H\underbrace{(\mathbf{F}_M\mathbf{X}\mathbf{F}_N^H)}_{\text{ISFFT}} = \mathbf{G}_{\mathrm{tx}}\mathbf{X}\mathbf{F}_N^H$$

- In vector form:

$$\mathbf{s} = \mathrm{vec}(\mathbf{S}) = (\mathbf{F}_N^H \otimes \mathbf{G}_{\mathrm{tx}})\mathbf{x}$$

- Received signal at delay–Doppler domain: pulse shaping+Wigner+SFFT on time–frequency received signal

$$\mathbf{Y} = \mathbf{F}_M^H(\mathbf{F}_M\mathbf{G}_{\mathrm{rx}}\mathbf{R})\mathbf{F}_N = \mathbf{G}_{\mathrm{rx}}\mathbf{R}\mathbf{F}_N$$

- In vector form:

$$\mathbf{y} = (\mathbf{F}_N \otimes \mathbf{G}_{\mathrm{rx}})\mathbf{r}$$

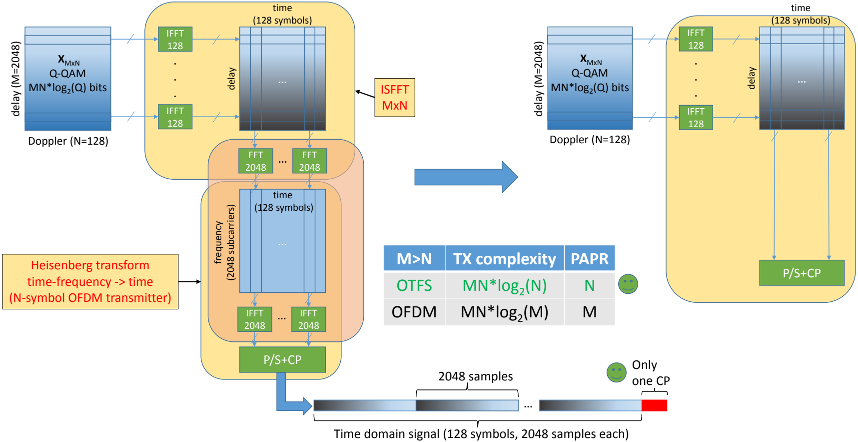

M>N	TX complexity	PAPR
OTFS	$MN*\log_2(N)$	N
OFDM	$MN*\log_2(M)$	M

- OTFS transmitter implements inverse ZAK transform (2D→1D)

OTFS receiver implementation: $M = 2048,\ N = 128$

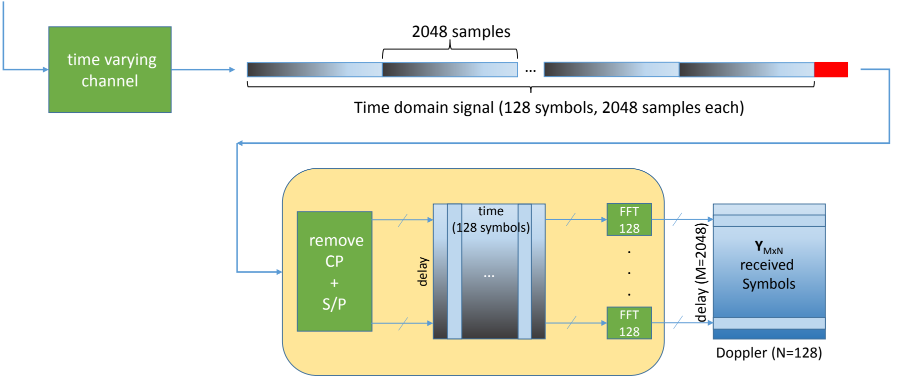

- OTFS receiver implements ZAK transform (1D→2D)

OTFS: matrix representation – channel

- Received signal in the time–frequency domain

$$r(t) = \int \int h(\tau, \nu) s(t-\tau) e^{j2\pi\nu(t-\tau)} d\tau d\nu + w(t)$$

- Channel

$$h(\tau, \nu) = \sum_{i=1}^{P} h_i \delta(\tau - \tau_i) \delta(\nu - \nu_i)$$

- Received signal in discrete form

$$r(n) = \sum_{i=1}^{P} h_i \underbrace{e^{\frac{j2\pi k_i (n-l_i)}{MN}}}_{\text{Doppler}} \underbrace{s([n-l_i]_{MN})}_{\text{Delay}} + w(n), 0 \le n \le MN-1$$

OTFS: matrix representation – channel

- Received signal in vector form

$$\mathbf{r} = \mathbf{H}\mathbf{s} + \mathbf{w}$$

- $\mathbf{H}$ is an $MN \times MN$ matrix of the following form

$$\mathbf{H} = \sum_{i=1}^{P} h_i \mathbf{\Pi}^{l_i} \mathbf{\Delta}^{(k_i)},$$

where, $\mathbf{\Pi}$ is the permutation matrix (forward cyclic shift), and $\mathbf{\Delta}^{(k_i)}$ is the diagonal matrix

$$\underbrace{\mathbf{\Pi} = \begin{bmatrix} 0 & \cdots & 0 & 1 \\ 1 & \ddots & 0 & 0 \\ \vdots & \ddots & \ddots & \vdots \\ 0 & \cdots & 1 & 0 \end{bmatrix}_{MN \times MN}}_{\text{Delay (similar to OFDM)}}, \underbrace{\mathbf{\Delta}^{(k_i)} = \begin{bmatrix} e^{\frac{j2\pi k_i(0)}{MN}} & 0 & \cdots & 0 \\ 0 & e^{\frac{j2\pi k_i(1)}{MN}} & \cdots & 0 \\ \vdots & & \ddots & \vdots \\ 0 & 0 & \cdots & e^{\frac{j2\pi k_i(MN-1)}{MN}} \end{bmatrix}}_{\text{Doppler}}$$

OTFS: matrix representation – channel

- Received signal at delay–Doppler domain

$$\mathbf{y} = \left[(\mathbf{F}_N \otimes \mathbf{G}_{\mathrm{rx}})\mathbf{H}(\mathbf{F}_N^H \otimes \mathbf{G}_{\mathrm{tx}})\right]\mathbf{x} + (\mathbf{F}_N \otimes \mathbf{G}_{\mathrm{rx}})\mathbf{w}$$
$$= \mathbf{H}_{\mathrm{eff}}\mathbf{x} + \widetilde{\mathbf{w}}$$

- Effective channel for arbitrary pulses

$$\mathbf{H}_{\mathrm{eff}} = (\mathbf{I}_N \otimes \mathbf{G}_{\mathrm{rx}})(\mathbf{F}_N \otimes \mathbf{I}_M)\mathbf{H}(\mathbf{F}_N^H \otimes \mathbf{I}_M)(\mathbf{I}_N \otimes \mathbf{G}_{\mathrm{tx}})$$
$$= (\mathbf{I}_N \otimes \mathbf{G}_{\mathrm{rx}}) \underbrace{\mathbf{H}_{\mathrm{eff}}^{\mathrm{rect}}} (\mathbf{I}_N \otimes \mathbf{G}_{\mathrm{tx}})$$

Channel for rectangular pulses ($\mathbf{G}_{\mathrm{tx}} = \mathbf{G}_{\mathrm{rx}} = \mathbf{I}_M$)

- Effective channel for rectangular pulses

$$\mathbf{H}_{\mathrm{eff}}^{\mathrm{rect}} = \sum_{i=1}^{P} h_i \underbrace{\left[(\mathbf{F}_N \otimes \mathbf{I}_M)\mathbf{\Pi}^{l_i}(\mathbf{F}_N^H \otimes \mathbf{I}_M)\right]}_{\mathbf{P}^{(i)}\ \text{(delay)}} \underbrace{\left[(\mathbf{F}_N \otimes \mathbf{I}_M)\mathbf{\Delta}^{(k_i)}(\mathbf{F}_N^H \otimes \mathbf{I}_M)\right]}_{\mathbf{Q}^{(i)}\ \text{(Doppler)}}$$

$$= \sum_{i=1}^{P} h_i \mathbf{P}^{(i)}\mathbf{Q}^{(i)} = \sum_{i=1}^{P} h_i \mathbf{T}^{(i)}$$

OTFS: Example for computing $\mathbf{H}_{\text{eff}}^{\text{rect}}$

- $M = 2,\ N = 2, MN = 4$
- $l_i = 0$ and $k_i = 0$ (no delay and Doppler)
  - $\mathbf{\Pi}^{l_i=0} = \mathbf{I}_4 \Rightarrow \mathbf{P}^{(i)} = (\mathbf{F}_2 \otimes \mathbf{I}_2)(\mathbf{F}_2^H \otimes \mathbf{I}_2) = \mathbf{I}_4$
  - $\mathbf{\Delta}^{(k_i=0)} = \mathbf{I}_4 \Rightarrow \mathbf{Q}^{(i)} = (\mathbf{F}_2 \otimes \mathbf{I}_2)(\mathbf{F}_2^H \otimes \mathbf{I}_2) = \mathbf{I}_4$
  - $\mathbf{T}^{(i)} = \mathbf{P}^{(i)}\mathbf{Q}^{(i)} = \mathbf{I}_4 \Rightarrow$ Narrowband channel

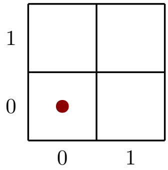

OTFS: Example for computing $\mathbf{H}_{\text{eff}}^{\text{rect}}$

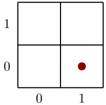

- $l_i = 1$ and $k_i = 0$ (delay but no Doppler)
  - $\mathbf{\Pi}^{l_i=1} = \begin{bmatrix} 0 & 0 & 0 & 1 \\ 1 & 0 & 0 & 0 \\ 0 & 1 & 0 & 0 \\ 0 & 0 & 1 & 0 \end{bmatrix} \Rightarrow$ block circulant matrix with 2×2 $(M \times M)$ block size
  - $\mathbf{P}^{(i)} = (\mathbf{F}_2 \otimes \mathbf{I}_2)\mathbf{\Pi}(\mathbf{F}_2^H \otimes \mathbf{I}_2) = \begin{bmatrix} 0 & 1 & 0 & 0 \\ 1 & 0 & 0 & 0 \\ 0 & 0 & 0 & e^{-j2\pi\frac{1}{2}} \\ 0 & 0 & 1 & 0 \end{bmatrix}$

    (using the block circulant matrix decomposition $\rightarrow$ generalization of circulant matrix decomposition in OFDM)
  - $\mathbf{\Delta}^{(k_i=0)} = \mathbf{I}_4 \Rightarrow \mathbf{Q}^{(i)} = (\mathbf{F}_2 \otimes \mathbf{I}_2)(\mathbf{F}_2^H \otimes \mathbf{I}_2) = \mathbf{I}_4$
  - $\mathbf{T}^{(i)} = \mathbf{P}^{(i)} \Rightarrow \mathbf{T}^{(i)}\mathbf{s} \rightarrow$ circularly shifts the elements in each block (size M) of $\mathbf{s}$ by 1 (delay shift)

OTFS: Example for computing $\mathbf{H}_{\text{eff}}^{\text{rect}}$

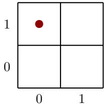

- $l_i = 0$ and $k_i = 1$ (Doppler but no delay)
  - $\mathbf{\Pi}^{l_i=0} = \mathbf{I}_4 \Rightarrow \mathbf{P}^{(i)} = (\mathbf{F}_2 \otimes \mathbf{I}_2)(\mathbf{F}_2^H \otimes \mathbf{I}_2) = \mathbf{I}_4$
  - $\mathbf{\Delta}^{(k_i=1)} = \begin{bmatrix} 1 & 0 & 0 & 0 \\ 0 & e^{j2\pi\frac{1}{4}} & 0 & 0 \\ 0 & 0 & e^{j2\pi\frac{2}{4}} & 0 \\ 0 & 0 & 0 & e^{j2\pi\frac{3}{4}} \end{bmatrix} \Rightarrow$ block diagonal matrix with 2×2 $(M \times M)$ block size
  - $\mathbf{Q}^{(i)} = (\mathbf{F}_2 \otimes \mathbf{I}_2)\mathbf{\Delta}^{(1)}(\mathbf{F}_2^H \otimes \mathbf{I}_2) = \begin{bmatrix} 0 & 0 & 1 & 0 \\ 0 & 0 & 0 & e^{j2\pi\frac{1}{4}} \\ 1 & 0 & 0 & 0 \\ 0 & e^{j2\pi\frac{1}{4}} & 0 & 0 \end{bmatrix}$
    (using the block circulant matrix decomposition in reverse direction)
  - $\mathbf{T}^{(i)} = \mathbf{Q}^{(i)} \Rightarrow \mathbf{T}^{(i)}\mathbf{s} \rightarrow$ circularly shifts the blocks (size M) of $\mathbf{s}$ by 1 (Doppler shift)

OTFS: Example for computing $\mathbf{H}_{\text{eff}}^{\text{rect}}$

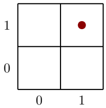

- $l_i = 1$ and $k_i = 1$ (both delay and Doppler)
  - $\mathbf{P}^{(i)} = \begin{bmatrix} 0 & 1 & 0 & 0 \\ 1 & 0 & 0 & 0 \\ 0 & 0 & 0 & e^{-j2\pi\frac{1}{2}} \\ 0 & 0 & 1 & 0 \end{bmatrix}$
  - $\mathbf{Q}^{(i)} = \begin{bmatrix} 0 & 0 & 1 & 0 \\ 0 & 0 & 0 & e^{j2\pi\frac{1}{4}} \\ 1 & 0 & 0 & 0 \\ 0 & e^{j2\pi\frac{1}{4}} & 0 & 0 \end{bmatrix}$
  - $\mathbf{T}^{(i)} = \mathbf{P}^{(i)}\mathbf{Q}^{(i)} \Rightarrow \mathbf{T}^{(i)}\mathbf{s} \rightarrow$ circularly shifts both the blocks (size M) and the elements in each block of $\mathbf{s}$ by 1 (delay and Doppler shifts)

OTFS: channel for rectangular pulses

- $\mathbf{T}^{(i)}$ has only one non-zero element in each row and the position and value of the non-zero element depends on the delay and Doppler values.

$$\mathbf{T}^{(i)}(p,q) = \begin{cases} e^{-j2\pi \frac{n}{N}} e^{j2\pi \frac{k_i([m-l_i]_M)}{MN}}, & \text{if } q = [m-l_i]_M + M[n-k_i]_N \text{ and } m < l_i \\ e^{j2\pi \frac{k_i([m-l_i]_M)}{MN}}, & \text{if } q = [m-l_i]_M + M[n-k_i]_N \text{ and } m \geq l_i \\ 0, & \text{otherwise.} \end{cases}$$

- Example: $l_i = 1$ and $k_i = 1$

$$\mathbf{T}^{(i)} = \begin{bmatrix} 0 & 0 & 0 & e^{j2\pi \frac{1}{4}} \\ 0 & 0 & 1 & 0 \\ 0 & e^{-j2\pi \frac{1}{4}} & 0 & 0 \\ 1 & 0 & 0 & 0 \end{bmatrix}$$

OTFS Signal Detection

Vectorized formulation of the input-output relation

- The input-output relation in the delay–Doppler domain is a 2D convolution (with i.i.d. additive noise $w[k, l]$)

$$y[k, l] = \sum_{i=1}^{P} h_i x[[k - k_{\nu_i}]_N, [l - l_{\tau_i}]_M] + w[k, l] \quad k = 1 \ldots N, l = 1 \ldots M \qquad (1)$$

- Detection of information symbols $x[k, l]$ requires a deconvolution operation i.e., the solution of the linear system of NM equations

$$\mathbf{y} = \mathbf{H}\mathbf{x} + \mathbf{w} \qquad (2)$$

where $\mathbf{x}, \mathbf{y}, \mathbf{w}$ are $x[k, l], y[k, l], w[k, l]$ in vectorized form and $\mathbf{H}$ is the $NM \times NM$ coefficient matrix of (1).

- Given the sparse nature of $\mathbf{H}$ we can solve (2) by using a message passing algorithm similar to (*)

(*) P. Som, T. Datta, N. Srinidhi, A. Chockalingam, and B. S. Rajan, "Low-complexity detection in large-dimension MIMO-ISI channels using graphical models," *IEEE J. Sel. Topics in Signal Processing*, vol. 5, no. 8, pp. 1497-1511, December 2011.

Message passing based detection

- Symbol-by-symbol MAP detection

$$\begin{aligned}\widehat{x}[c] &= \arg\max_{a_j \in \mathbb{A}} \Pr\left(x[c] = a_j \,\middle|\, \mathbf{y}, \mathbf{H}\right) \\ &= \arg\max_{a_j \in \mathbb{A}} \frac{1}{Q} \Pr\left(\mathbf{y} \,\middle|\, x[c] = a_j, \mathbf{H}\right) \\ &\approx \arg\max_{a_j \in \mathbb{A}} \prod_{d \in \mathcal{J}_c} \Pr\left(y[d] \,\middle|\, x[c] = a_j, \mathbf{H}\right)\end{aligned}$$

- Received signal $y[d]$

$$y[d] = x[c]H[d,c] + \underbrace{\sum_{e \in \mathcal{I}(d), e \neq c} x[e]H[d,e] + z[d]}_{\zeta_{d,c}^{(i)} \rightarrow \text{ assumed to be Gaussian}}$$

Messages in factor graph

Algorithm 1 MP algorithm for OTFS symbol detection

Input: Received signal $\mathbf{y}$, channel matrix $\mathbf{H}$

Initialization: pmf $\mathbf{p}_{c,d}^{(0)} = 1/Q$ **repeat**

- Observation nodes send the mean and variance to variable nodes
- Variable nodes send the pmf to the observation nodes
- Update the decision

until *Stopping criteria*;

Output: The decision on transmitted symbols $\widehat{x}[c]$

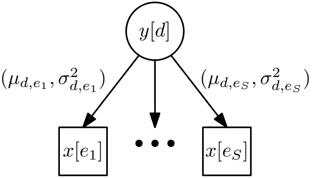

$\{e_1, e_2, \cdots, e_S\} = \mathcal{I}_d$

Observation node messages

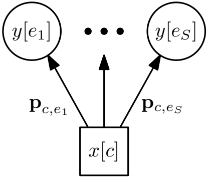

$\{e_1, e_2, \cdots, e_S\} = \mathcal{J}_c$

Variable node messages

Messages in factor graph – observation node messages

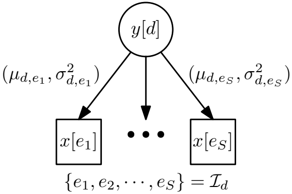

- Received signal

$$y[d] = x[c]H[d,c] + \underbrace{\sum_{e\in\mathcal{I}(d),e\neq c} x[e]H[d,e] + z[d]}_{\zeta^{(i)}_{d,c} \rightarrow \text{ assumed to be Gaussian}}$$

- Mean and Variance

$$\mu^{(i)}_{d,c} = \sum_{e\in\mathcal{I}(d),e\neq c} \sum_{j=1}^{Q} p^{(i-1)}_{e,d}(a_j)a_j H[d,e]$$

$$(\sigma^{(i)}_{d,c})^2 = \sum_{e\in\mathcal{I}(d),e\neq c} \left(\sum_{j=1}^{Q} p^{(i-1)}_{e,d}(a_j)|a_j|^2 |H[d,e]|^2 - \left| \sum_{j=1}^{Q} p^{(i-1)}_{e,d}(a_j)a_j H[d,e] \right|^2 \right) + \sigma^2$$

Messages in factor graph – variable node messages

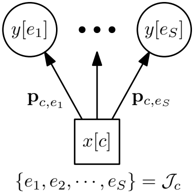

- Probability update with damping factor Δ

$$p_{c,d}^{(i)}(a_j) = \Delta \cdot \tilde{p}_{c,d}^{(i)}(a_j) + (1-\Delta) \cdot p_{c,d}^{(i-1)}(a_j), a_j \in \mathbb{A}$$

where

$$\tilde{p}_{c,d}^{(i)}(a_j) \propto \prod_{e \in \mathcal{J}(c), e \neq d} \Pr\left(y[e] \middle| x[c] = a_j, \mathbf{H}\right)$$

$$= \prod_{e \in \mathcal{J}(c), e \neq d} \frac{\xi^{(i)}(e,c,j)}{\sum_{k=1}^{Q} \xi^{(i)}(e,c,k)}$$

$$\xi^{(i)}(e,c,k) = \exp\left(\frac{-\left|y[e] - \mu_{e,c}^{(i)} - H_{e,c} a_k\right|^2}{(\sigma_{e,c}^{(i)})^2}\right)$$

Final update and stopping criterion

- Final update

$$p_c^{(i)}(a_j) = \prod_{e \in \mathcal{J}(c)} \frac{\xi^{(i)}(e,c,j)}{\sum_{k=1}^{Q} \xi^{(i)}(e,c,k)}$$

$$\widehat{x}[c] = \arg\max_{a_j \in \mathbb{A}} \; p_c^{(i)}(a_j), \quad c = 1, \cdots, NM.$$

- Stopping Criterion
  - Convergence Indicator $\eta^{(i)} = 1$

$$\eta^{(i)} = \frac{1}{NM} \sum_{c=1}^{NM} \mathbb{I}\left(\max_{a_j \in \mathbb{A}} \; p_c^{(i)}(a_j) \geq 0.99 \right)$$

  - Maximum number of Iterations
- Complexity (linear) – $\mathcal{O}(n_{iter} SQ)$ per symbol which is much less even compared to a linear MMSE detector $\mathcal{O}((NM)^2)$

Simulation results – damping factor Δ

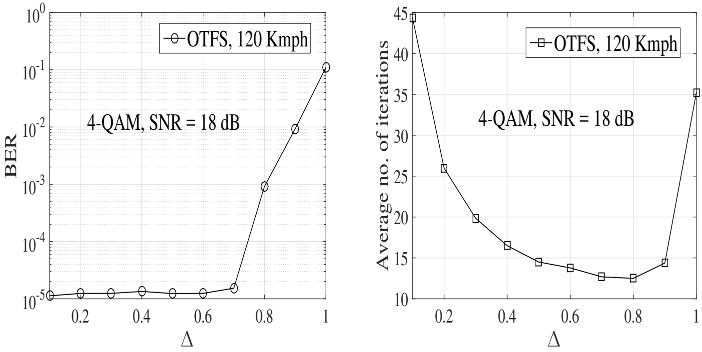

Figure: Variation of BER and average iterations no. with Δ. Optimal for $\Delta = 0.7$

Simulation results – OTFS vs OFDM with ideal pulses

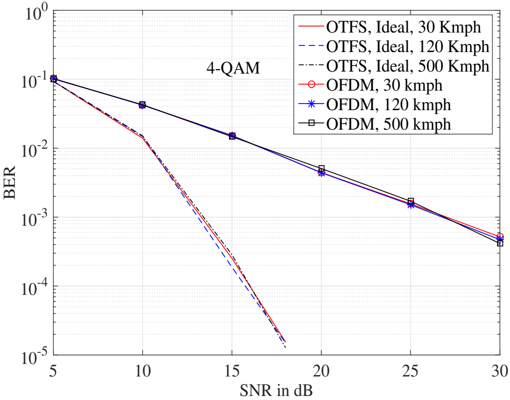

Figure: The BER performance comparison between OTFS with ideal pulses and OFDM systems at different Doppler frequencies.

Simulation results – IDI effect

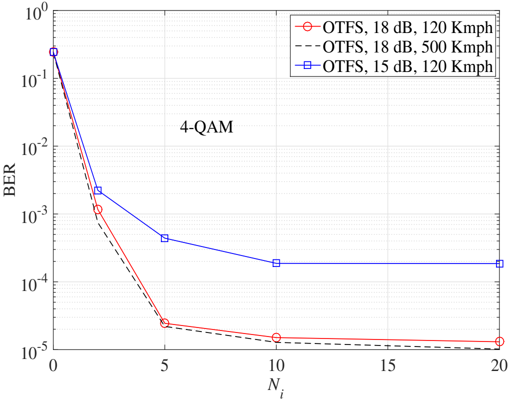

Figure: The BER performance of OTFS for different number of interference terms N_i with 4-QAM.

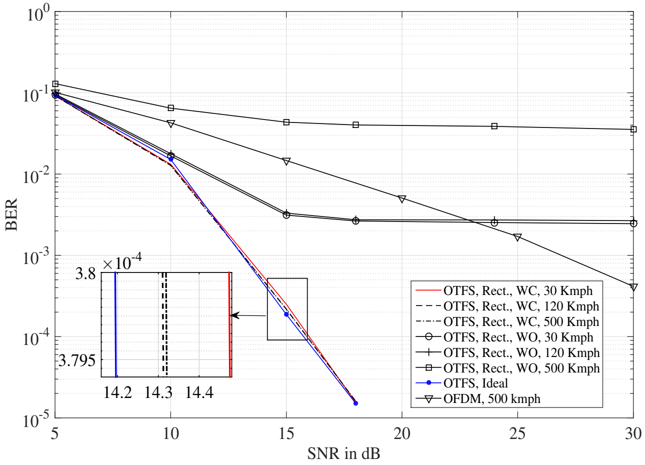

Figure: The BER performance of OTFS with rectangular and ideal pulses at different Doppler frequencies for 4-QAM.

Simulation results – Ideal and Rect. pulses - 16-QAM

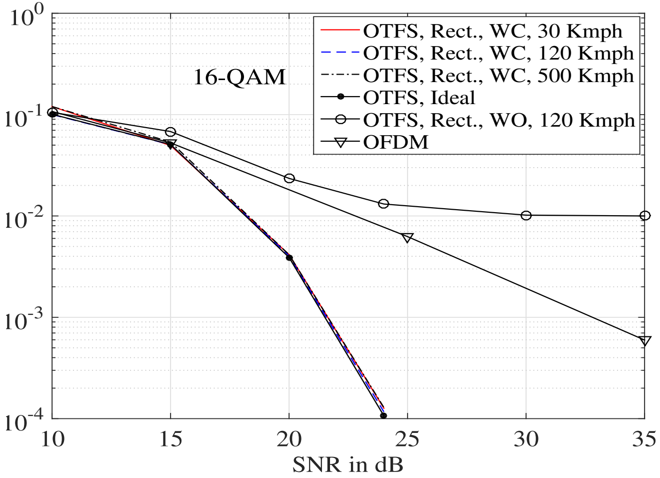

Figure: The BER performance of OTFS with rectangular and ideal pulses at different Doppler frequencies for 16-QAM.

Simulation results – Low latency

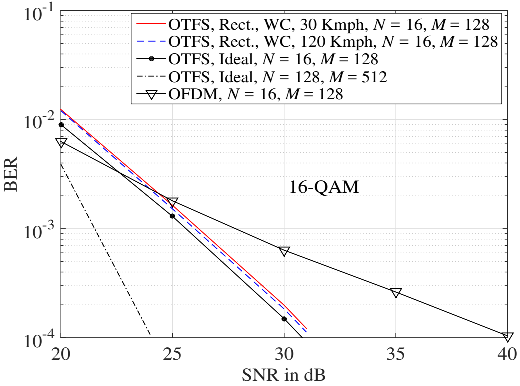

Figure: The BER performance of OTFS with rectangular pulses and low latency ($N = 16$, $T_f \approx 1.1$ ms).

Matlab code

- OTFS_sample_code.m

→ OTFS_modulation – 1. ISFFT, 2. Heisenberg transform

```
X = fft(ifft(x).').'/sqrt(M/N); % ISFFT
s_mat = ifft(X.')*sqrt(M); % Heisenberg transform
s = s_mat(:);
```

→ OTFS_channel_gen – generates wireless channel

output: (delay_taps,Doppler_taps,chan_coef)

→ OTFS_channel_output – wireless channel and noise

```
L = max(delay_taps);
s = [s(N*M-L+1:N*M);s];% add one cp
s_chan = 0;
for itao = 1:taps
    s_chan = s_chan+chan_coef(itao)*circshift([s.*exp(1j*2*pi/M...
    *(-L:-L+length(s)-1)*Doppler_taps(itao)/N).';zeros(L,1)],delay_taps(itao));
end
noise = sqrt(sigma_2/2)*(randn(size(s_chan)) + 1i*randn(size(s_chan)));
r = s_chan + noise;
r = r(L+1:L+(N*M));% discard cp
```

Matlab code

→ OTFS_demodulation – 1. Wiegner transform, 2. SFFT

```
r_mat = reshape(r,M,N);
Y = fft(r_mat)/sqrt(M); % Wigner transform
Y = Y.';
y = ifft(fft(Y).').'/sqrt(N/M); % SFFT
```

→ OTFS_mp_detector – message passing detector

Other detection methods

- Output OTFS signal: $\mathbf{y} = \mathbf{H}\mathbf{x} + \mathbf{w}$

1. MMSE detection:

$$\hat{\mathbf{x}} = \left(\mathbf{H}^H\mathbf{H} + \lambda\mathbf{I}\right)^{-1}\mathbf{H}^H\mathbf{y}$$

   - Provides diversity but high complex $\mathcal{O}((NM)^3)$

2. OTFS FDE (frequency domain equalization) in [1]
   - Equalization in time–frequency domain (one-tap) and apply the SFFT
   - Low complexity equalizer
   - Phase shifts can't be applied and bad performance at high Dopplers
   - Small improvement on OFDM

---

[1]. Li Li, H. Wei, Y. Huang, Y. Yao, W. Ling, G. Chen, P. Li, and Y. Cai, "A simple two-stage equalizer With simplified orthogonal time frequency space modulation over rapidly time-varying channels," available online: https://arxiv.org/abs/1709.02505.

Other detection methods

3. OTFS MMSE-PIC (parallel ISI cancellation) in [2]
   - First applies the equalization in time–frequency domain (one-tap) and then applies successive cancellation with coding
   - Successive cancellation

$$\hat{\mathbf{y}}(i)_{j+1} = \mathbf{y} - \mathbf{H}\hat{\mathbf{x}}_j + \mathbf{H}(:, i)\hat{\mathbf{x}}(i)_j$$

$$\hat{\mathbf{x}}(i)_{j+1} = \arg\min_{a \in \mathcal{A}} \left(\hat{\mathbf{y}}(i)_{j+1} - \mathbf{H}(:, i)a \right)$$

   - Moderate complexity
   - Better performance than [1] but still struggles with the high Doppler
4. MCMC sampling [3]
   - Approximate ML solution using Gibbs sampling based MCMC technique
   - High complexity $\mathcal{O}(n_{iter}NM)$ compared to message passing ($\mathcal{O}(n_{iter}SQ)$) (Does not take advantage of sparsity of the channel matrix)

[2]. T. Zemen, M. Hofer, and D. Loeschenbrand, "Low-complexity equalization for orthogonal time and frequency signaling (OTFS)," available online: https://arxiv.org/pdf/1710.09916.pdf.

[3]. K. R. Murali and A. Chockalingam, "On OTFS modulation for high-Doppler fading channels," in *Proc. ITA'2018,* San Diego, Feb. 2018.

MIMO/multiuser MIMO OTFS

MIMO-OTFS modulation

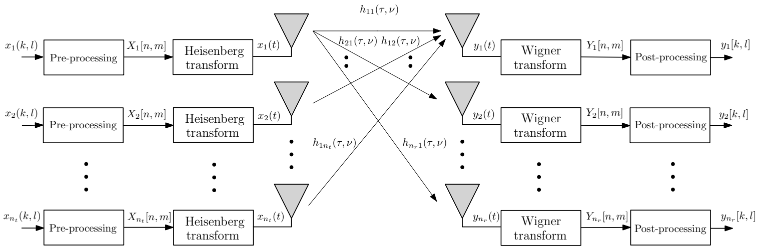

Figure: Block diagram of MIMO-OTFS modulation scheme

- n_t - number of transmit antennas, n_r - number of receive antennas
- Assume that the channel corresponding to pth transmit antenna and qth receive antenna is given by

$$h_{qp}(\tau,\nu) = \sum_{i=1}^{P} h_{qp_i}\delta(\tau-\tau_i)\delta(\nu-\nu_i),$$

$p = 1, 2, \cdots, n_t,\ q = 1, 2, \cdots, n_r$

Vectorized formulation of input-output relation

- Let the windows $W_{tx}[n, m]$, $W_{rx}[n, m]$ used for modulation be rectangular
- $\mathbf{H}_{qp}$ - equivalent channel matrix corresponding to pth transmit antenna and qth receive antenna
- $\mathbf{x}_p$ - $NM \times 1$ transmit vector from the pth transmit antenna in a given frame
- $\mathbf{y}_q$ - $NM \times 1$ received vector corresponding to qth receive antenna in a given frame
- Input-output relationship for the MIMO-OTFS system

$$
\begin{aligned}
\mathbf{y}_1 &= \mathbf{H}_{11}\mathbf{x}_1 + \mathbf{H}_{12}\mathbf{x}_2 + \cdots + \mathbf{H}_{1n_t}\mathbf{x}_{n_t} + \mathbf{v}_1 \\
\mathbf{y}_2 &= \mathbf{H}_{21}\mathbf{x}_1 + \mathbf{H}_{22}\mathbf{x}_2 + \cdots + \mathbf{H}_{2n_t}\mathbf{x}_{n_t} + \mathbf{v}_2 \\
&\vdots \\
\mathbf{y}_{n_r} &= \mathbf{H}_{n_r1}\mathbf{x}_1 + \mathbf{H}_{n_r2}\mathbf{x}_2 + \cdots + \mathbf{H}_{n_rn_t}\mathbf{x}_{n_t} + \mathbf{v}_{n_r}
\end{aligned}
$$

- Define

$$\mathbf{H}_{\text{MIMO}} = \begin{bmatrix} \mathbf{H}_{11} & \mathbf{H}_{12} & \dots & \mathbf{H}_{1n_t} \\ \mathbf{H}_{21} & \mathbf{H}_{22} & \dots & \mathbf{H}_{2n_t} \\ \vdots & \vdots & \ddots & \vdots \\ \mathbf{H}_{n_r1} & \mathbf{H}_{n_r2} & \dots & \mathbf{H}_{n_rn_t} \end{bmatrix},$$

$$\mathbf{x}_{\text{MIMO}} = [\mathbf{x}_1{}^T, \mathbf{x}_2{}^T, \cdots, \mathbf{x}_{n_t}{}^T]^T, \mathbf{y}_{\text{MIMO}} = [\mathbf{y}_1{}^T, \mathbf{y}_2{}^T, \cdots, \mathbf{y}_{n_r}{}^T]^T,$$
$$\mathbf{v}_{\text{MIMO}} = [\mathbf{v}_1{}^T, \mathbf{v}_2{}^T, \cdots, \mathbf{v}_{n_r}{}^T]^T.$$

- Linear system model, $\mathbf{y}_{\text{MIMO}} = \mathbf{H}_{\text{MIMO}}\mathbf{x}_{\text{MIMO}} + \mathbf{v}_{\text{MIMO}}$
- $\mathbf{x}_{\text{MIMO}} \in \mathbb{C}^{n_tNM\times 1}, \mathbf{y}_{\text{MIMO}}, \mathbf{v}_{\text{MIMO}} \in \mathbb{C}^{n_rNM\times 1}$, $\mathbf{H}_{\text{MIMO}} \in \mathbb{C}^{n_rNM\times n_tNM}$
- Only n_tP non-zero elements in each row and n_rP non-zero elements in each column of $\mathbf{H}_{\text{MIMO}}$

Vectorized formulation of input-output relation for MIMO-OFDM

- $\mathbf{H}_{\text{OFDM}_{qp}}$ - the equivalent channel matrix corresponding to pth transmit antenna and qth receive antenna
- $\mathbf{x}_{\text{OFDM}_p}$ - $NM \times 1$ transmit vector from the pth transmit antenna in a given frame
- $\mathbf{y}_{\text{OFDM}_q}$ denote the $NM \times 1$ received vector corresponding to qth receive antenna in a given frame
- Define

$$\mathbf{H}_{\text{MIMO-OFDM}} = \begin{bmatrix} \mathbf{H}_{\text{OFDM}_{11}} & \mathbf{H}_{\text{OFDM}_{12}} & \cdots & \mathbf{H}_{\text{OFDM}_{1n_t}} \\ \mathbf{H}_{\text{OFDM}_{21}} & \mathbf{H}_{\text{OFDM}_{22}} & \cdots & \mathbf{H}_{\text{OFDM}_{2n_t}} \\ \vdots & \vdots & \ddots & \vdots \\ \mathbf{H}_{\text{OFDM}_{n_r1}} & \mathbf{H}_{\text{OFDM}_{n_r2}} & \cdots & \mathbf{H}_{\text{OFDM}_{n_rn_t}} \end{bmatrix}$$

- Define

$$\mathbf{x}_{\text{MIMO-OFDM}} = [\mathbf{x}_{\text{OFDM}_1}{}^T, \mathbf{x}_{\text{OFDM}_2}{}^T, \cdots, \mathbf{x}_{\text{OFDM}_{n_t}}{}^T]^T,$$
$$\mathbf{y}_{\text{MIMO-OFDM}} = [\mathbf{y}_{\text{OFDM}_1}{}^T, \mathbf{y}_{\text{OFDM}_2}{}^T, \cdots, \mathbf{y}_{\text{OFDM}_{n_r}}{}^T]^T$$

- Linear system model, $\mathbf{y}_{\text{MIMO-OFDM}} = \mathbf{H}_{\text{MIMO-OFDM}}\mathbf{x}_{\text{MIMO-OFDM}} + \mathbf{v}_{\text{MIMO-OFDM}}$
- $\mathbf{x}_{\text{MIMO-OFDM}} \in \mathbb{C}^{n_t NM \times 1}$, $\mathbf{y}_{\text{MIMO-OFDM}}, \mathbf{v}_{\text{MIMO-OFDM}} \in \mathbb{C}^{n_r NM \times 1}$, $\mathbf{H}_{\text{MIMO-OFDM}} \in \mathbb{C}^{n_r NM \times n_t NM}$

Performance results

- $\kappa_{\nu_i} = 0$ (no IDI) is assumed
- Delay and Doppler models

Path index (i)	1	2	3	4	5
Delay (τ_i,μs)	2.1	4.2	6.3	8.4	10.4
Doppler (ν_i,Hz)	0	470	940	1410	1880

- Simulation parameters

Parameter	**Value**
Carrier frequency (GHz)	4
Subcarrier spacing (kHz)	15
Frame size (M, N)	$(32, 32)$
Modulation scheme	BPSK
MIMO configuration	1×1, 1×2, 1×3, 2×2, 3×3, 2×3
Maximum speed (kmph)	507.6

Table: System parameters.

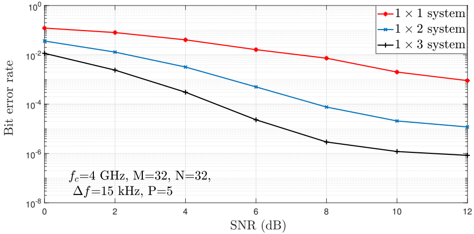

Figure: SISO, 1×2, 1×3

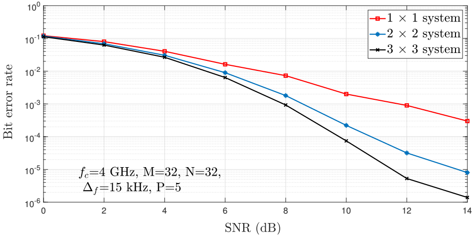

Figure: SISO, 2×2, 3×3

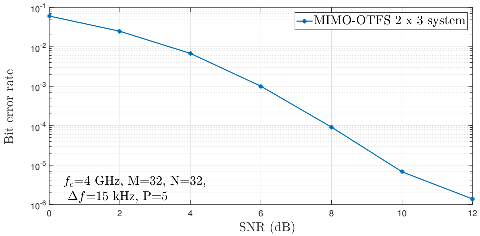

Figure: 2 × 3 system

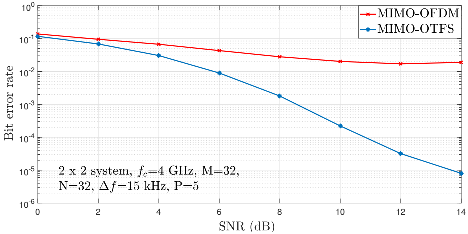

Figure: BER performance comparison between OTFS and OFDM

OTFS channel estimation

Channel estimation in time–frequency domain

- (l_{τ_i}, k_{ν_i}) ((delay,Doppler)) values are obtained from the baseband time domain signal equation

$$y(t) = \sum_{i=1}^{P} h_i x(t - \tau_i) e^{j2\pi\nu_i(t-\tau_i)}$$

- PN based pilots and 2D matched filter matrix is used to determine (l_{τ_i}, k_{ν_i})
- Highly complex

1. A. Fish, S. Gurevich, R. Hadani, A. M. Sayeed, and O. Schwartz, "Delay-Doppler channel estimation in almost linear complexity," *IEEE Trans. Inf. Theory,* vol. 59, no. 11, pp. 7632-7644, Nov. 2013.
2. K. R. Murali, and A. Chockalingam, "On OTFS modulation for high-Doppler fading channels," in *Proc. ITA'2018,* San Diego, Feb. 2018.

Channel estimation using impulses in the delay-Doppler domain

- Each transmit and receive antenna pair sees a different channel having a finite support in the delay-Doppler domain
- The support is determined by the delay and Doppler spread of the channel
- The OTFS input-output relation for pth transmit antenna and qth receive antenna pair can be written as

$$\hat{x}_q[k,l] = \sum_{m=0}^{M-1}\sum_{n=0}^{N-1} x_p[n,m]\frac{1}{MN} h_{w_{qp}}\left(\frac{k-n}{NT}, \frac{l-m}{M\Delta f}\right) + v_q[k,l].$$

1. P. Raviteja, K.T. Phan, and Y. Hong, "Embedded Pilot-Aided Channel Estimation for OTFS in Delay-Doppler Channels", *IEEE Trans. on Veh. Tech.*, March 2019 (Early Access).
2. M. K. Ramachandran and A. Chockalingam, "MIMO-OTFS in high-Doppler fading channels: Signal detection and channel estimation," available online: https://arxiv.org/abs/1805.02209.
3. R. Hadani and S. Rakib, "OTFS methods of data channel characterization and uses thereof." U.S. Patent 9 444 514 B2, Sept. 13, 2016.

- If we transmit

$$x_p[n,m] = 1 \text{ if } (n,m) = (n_p, m_p)$$
$$= 0 \ \forall \ (n,m) \neq (n_p, m_p),$$

as pilot from the pth antenna, the received signal at the qth antenna will be

$$\hat{x}_q[k,l] = \frac{1}{MN} h_{w_{qp}} \left(\frac{k - n_p}{NT}, \frac{l - m_p}{M\Delta f} \right) + v_q[k,l].$$

- $\frac{1}{MN} h_{w_{qp}} \left(\frac{k}{NT}, \frac{l}{M\Delta f} \right)$ and thus $\hat{\mathbf{H}}_{qp}$ can be estimated , since n_p and m_p are known at the receiver a priori
- Impulse at $(n,m) = (n_p, m_p)$ spreads only to the extent of the support of the channel in the delay-Doppler domain (2D convolution)
- If the pilot impulses have sufficient spacing in the delay-Doppler domain, they will be received without overlap

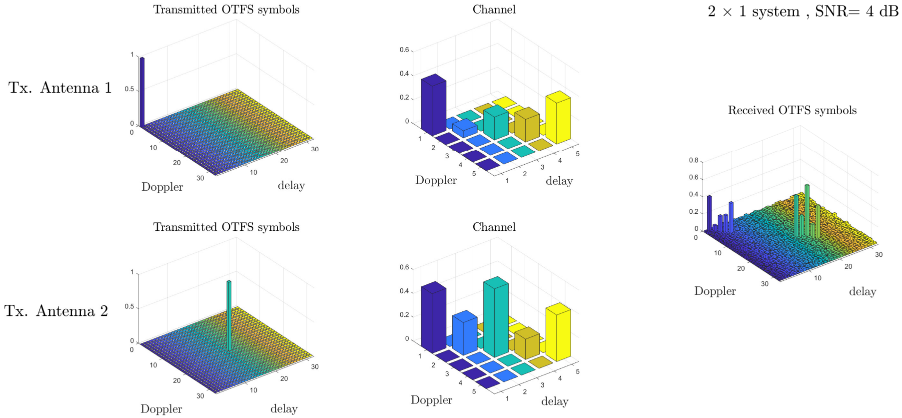

Figure: Illustration of pilots and channel response in delay-Doppler domain in a 2×1 MIMO-OTFS system

SISO OTFS system with integer Doppler

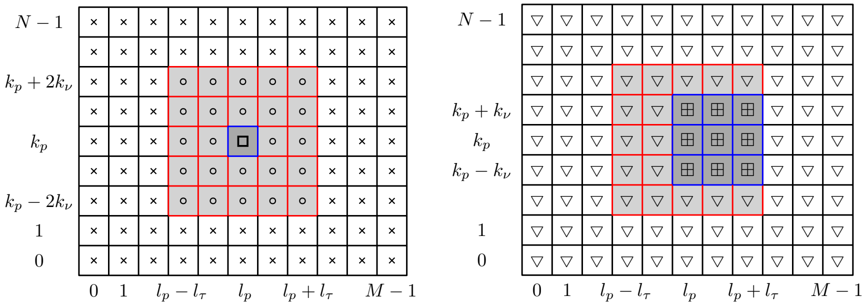

(a) Tx symbol arrangement (□: pilot; ○: guard symbols; ×: data symbols)

(b) Rx symbol pattern (▽: data detection, ⊞: channel estimation)

Figure: Tx pilot, guard, and data symbols and Rx received symbols

SISO OTFS system with fractional Doppler

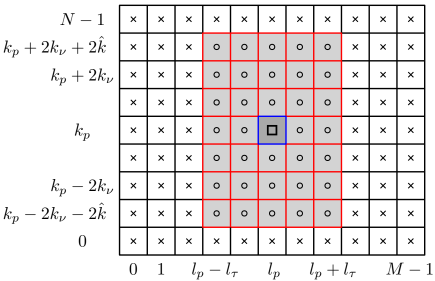

(a) Tx symbol arrangement (□: pilot; ∘: guard symbols; ×: data symbols)

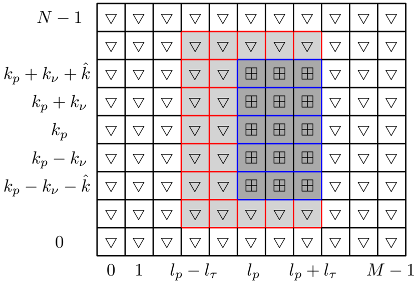

(b) Rx symbol pattern (▽: data detection, ⊞: channel estimation)

Figure: Tx pilot, guard, and data symbols and Rx received symbols

MIMO OTFS system with fractional Doppler

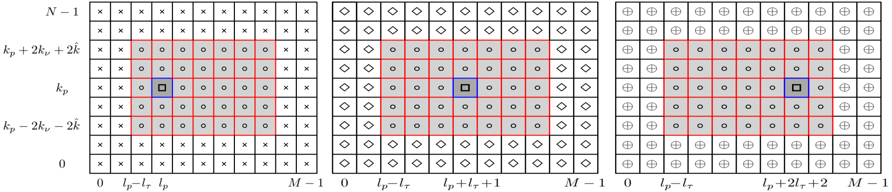

(a) Antenna 1 (×: antenna 1 data symbol)

(b) Antenna 2 (◊: antenna 2 data symbol)

(c) Antenna 3 (⊕: antenna 3 data symbol)

Figure: Tx pilot, guard, and data symbols for MIMO OTFS system (□: pilot; ○: guard)

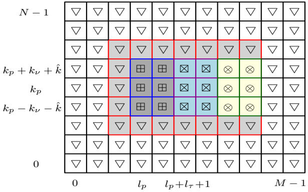

Figure: Rx symbol pattern at antenna 1 of MIMO OTFS system (▽: data detection, ⊞, ⊠, ⊗: channel estimation for Tx antenna 1, 2, and 3, respectively)

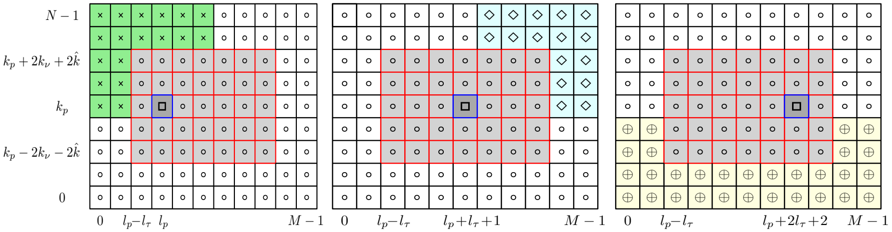

(a) User 1 ($\times$: user 1 data symbol)

(b) User 2 ($\Diamond$: user 2 data symbol)

(c) User 3 ($\oplus$: user 3 data symbol)

Figure: Tx pilot, guard, and data symbols for multiuser uplink OTFS system ($\square$: pilot; $\circ$: guard symbols)

SISO-OTFS performance with the estimated channel

- Simulation parameters: Carrier frequency of 4GHz, sub-carrier spacing of 15KHz, $M = 512$, $N = 128$, 4-QAM signaling, LTE EVA channel model
- Let SNR_p and SNR_d denote the average pilot and data SNRs
- Channel estimation threshold is $3\sigma_p$, where $\sigma_p^2 = 1/SNR_p$ is effective noise power of the pilot signal

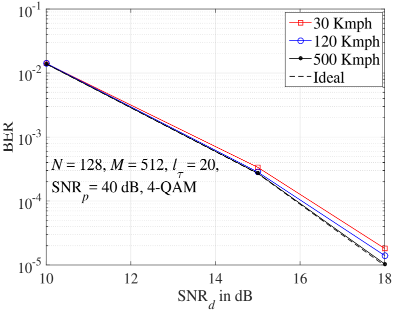

(a) BER for estimated channels of different Integer Dopplers

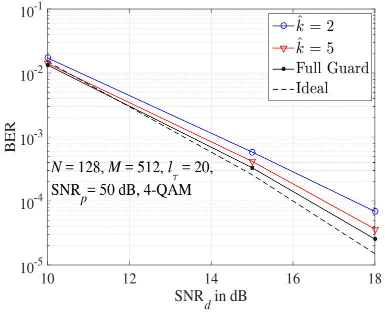

(b) BER for estimated channels of Fractional Doppler

OTFS applications

OTFS in radar application

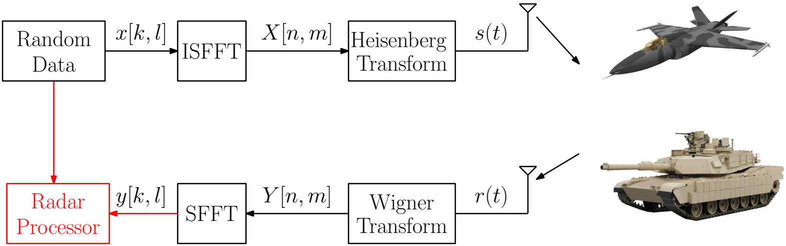

Figure: OTFS-based radar system architecture

- Received signal in delay–Doppler domain

$$\mathbf{y} = \widetilde{\mathbf{X}}\mathbf{h} + \mathbf{w}$$

- Estimated range and velocity (range↔delay & velocity↔Doppler) : Matched Filter

$$\hat{\mathbf{h}} = \widetilde{\mathbf{X}}^H\mathbf{y} = \widetilde{\mathbf{X}}^H\widetilde{\mathbf{X}}\mathbf{h} + \widetilde{\mathbf{X}}^H\mathbf{w} = \mathbf{G}\mathbf{h} + \widetilde{\mathbf{w}} \approx MNP_S\mathbf{h} + \widetilde{\mathbf{w}}$$

OTFS in radar application

- Target range and velocity: 975 m and 80 m/s

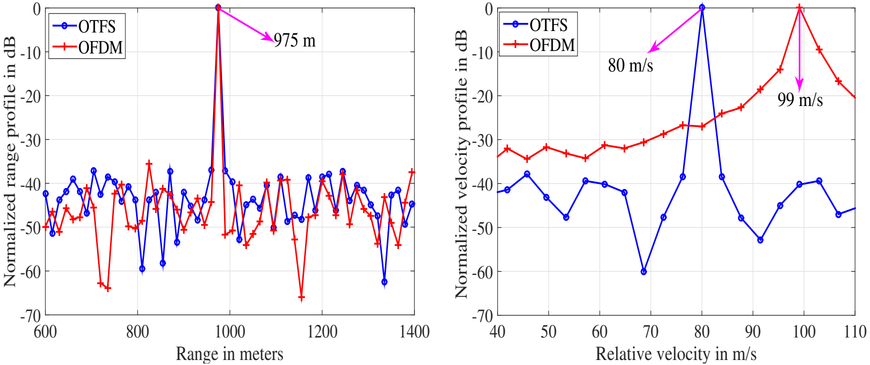

(a) range profile (b) velocity profile

Figure: OTFS vs OFDM radar

(*) P. Raviteja, K.T. Phan, Y. Hong, and E. Viterbo, "Orthogonal time frequency space (OTFS) modulation based radar system," accepted in *Radar Conference*, Boston, USA, April 2019.

OTFS modem SDR implementation block diagram

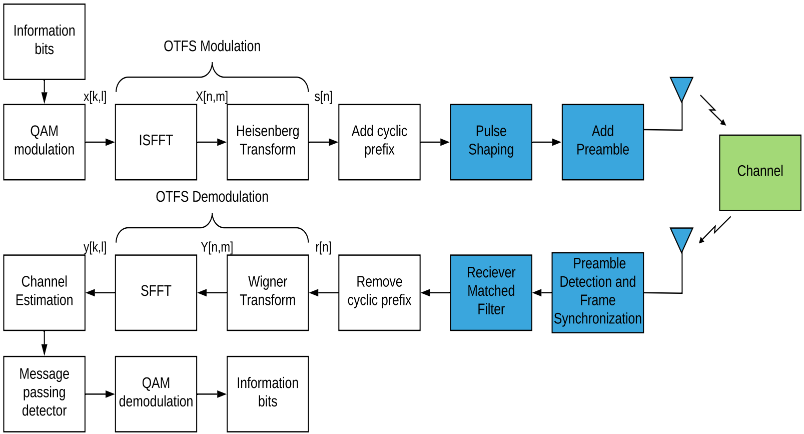

Experiment setup and parameters

- The wireless propagation channel can be observed in real time using LabView GUI at the RX while receiving the OTFS frames.

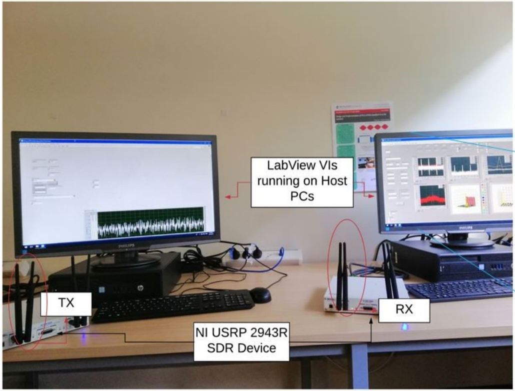

TABLE I
EXPERIMENT PARAMETERS

Symbol	Parameter	Value
f_c	Carrier frequency	4 GHz
M	Number of subcarriers	32
N	Number of symbols	32
Q	Modulation alphabet size	4,16
T	Symbol Time	1.28 micro secs
Δf	Subcarrier spacing	781.25 KHz
$1/M\Delta f$	delay resolution	40 nano secs
$1/NT$	Doppler resolution	24.4 KHz
Fd_{max}	Maximum Doppler spread	400KHz
d	Tx-Rx Distance	1.5 meters

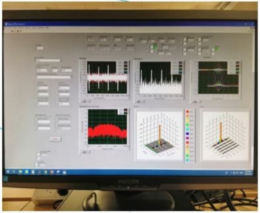

OTFS received pilot in a real indoor wireless channel

- DC Offset manifests itself as a constant signal in the delay-Doppler plane shifted by Doppler equal to CFO.

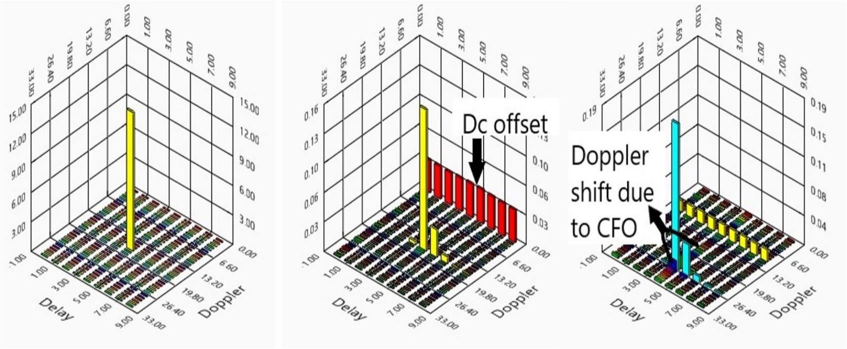

OTFS received pilot in a partially emulated indoor mobile channel

- Doppler paths were added to the TX OTFS waveform and transmitted it into a real indoor wireless channel for a time selective channel.

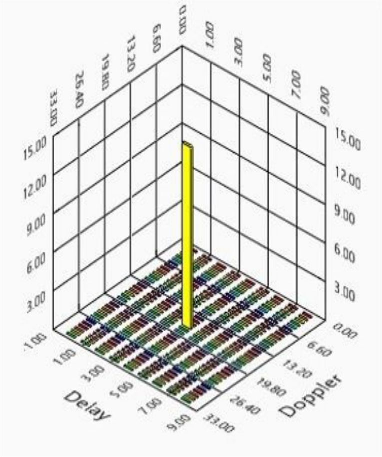

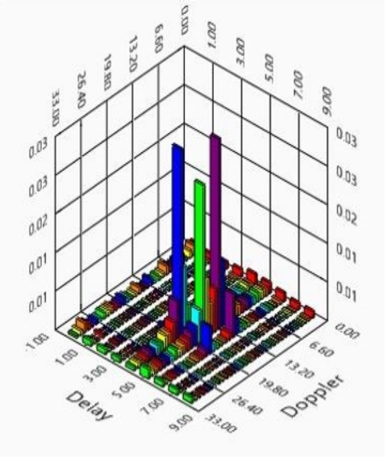

Error performance

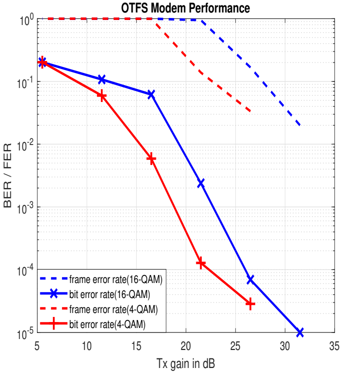

OTFS with static multipath channels (zero Doppler)

- Received signal

$$\text{(size } MN \times 1) \ \mathbf{y} = (\mathbf{F}_N \otimes \mathbf{I}_M)\mathbf{H}(\mathbf{F}_N^H \otimes \mathbf{I}_M)\mathbf{x} + \widetilde{\mathbf{w}}$$

$\downarrow$ zero Doppler

$$\text{(size } M \times 1) \ \mathbf{y}_n = \breve{\mathbf{H}}_n \mathbf{x}_n + \widetilde{\mathbf{w}}_n, \text{for } n = 0, \cdots, N-1$$

- Equivalent to A-OFDM (asymmetric OFDM) in (*)
- $\breve{\mathbf{H}}_n$ structure for $M \geq L$

$$\breve{\mathbf{H}}_n = \begin{bmatrix} h_0 & 0 & \cdots & h_1 e^{-j2\pi\frac{n}{N}} \\ h_1 & h_0 & \cdots & h_2 e^{-j2\pi\frac{n}{N}} \\ \vdots & \ddots & \ddots & \vdots \\ 0 & \cdots & h_1 & h_0 \end{bmatrix}_{M \times M}$$

- Achieves maximum diversity when $M \geq L$ (max. delay)
$\Longleftrightarrow$ N parallel CPSC transmissions each of length M

(*) J. Zhang, A. D. S. Jayalath, and Y. Chen, "Asymmetric OFDM systems based on layered FFT structure," *IEEE Signal Proces. Lett.*, vol. 14, no. 11, pp. 812-815, Nov. 2007.

OTFS with static multipath channels (zero Doppler)

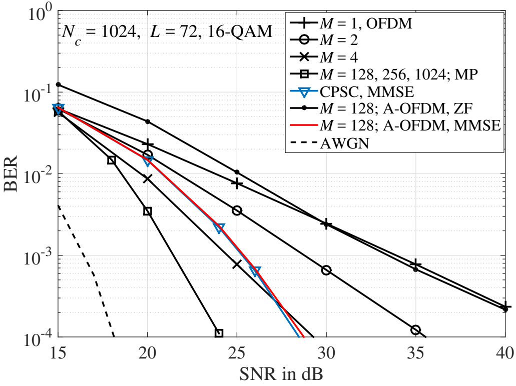

Figure: BER of OTFS for different M with $MN = N_c = 1024$, $L = 72$, and 16-QAM

(*) P. Raviteja, Y. Hong, and E. Viterbo, "OTFS performance on static multipath channels," *IEEE Wireless Commun. Lett.*, Jan. 2019, doi: 10.1109/LWC.2018.2890643.

References I

1. R. Hadani, S. Rakib, M. Tsatsanis, A. Monk, A. J. Goldsmith, A. F. Molisch, and R. Calderbank, "Orthogonal time frequency space modulation," in *Proc. IEEE WCNC*, San Francisco, CA, USA, March 2017.
2. R. Hadani, S. Rakib, S. Kons, M. Tsatsanis, A. Monk, C. Ibars, J. Delfeld, Y. Hebron, A. J. Goldsmith, A.F. Molisch, and R. Calderbank, "Orthogonal time frequency space modulation," Available online: https://arxiv.org/pdf/1808.00519.pdf.
3. R. Hadani, and A. Monk, "OTFS: A new generation of modulation addressing the challenges of 5G," *OTFS Physics White Paper*, Cohere Technologies, 7 Feb. 2018. Available online: https://arxiv.org/pdf/1802.02623.pdf.
4. R. Hadani et al., "Orthogonal Time Frequency Space (OTFS) modulation for millimeter-wave communications systems," 2017 IEEE MTT-S International Microwave Symposium (IMS), Honolulu, HI, 2017, pp. 681-683.
5. A. Fish, S. Gurevich, R. Hadani, A. M. Sayeed, and O. Schwartz, "Delay-Doppler channel estimation in almost linear complexity," *IEEE Trans. Inf. Theory*, vol. 59, no. 11, pp. 7632–7644, Nov 2013.
6. A. Monk, R. Hadani, M. Tsatsanis, and S. Rakib, "OTFS - Orthogonal time frequency space: A novel modulation technique meeting 5G high mobility and massive MIMO challenges." Technical report. Available online: https://arxiv.org/ftp/arxiv/papers/1608/1608.02993.pdf.

References II

7. R. Hadani and S. Rakib. “OTFS methods of data channel characterization and uses thereof.” U.S. Patent 9 444 514 B2, Sept. 13, 2016.
8. P. Raviteja, K. T. Phan, Q. Jin, Y. Hong, and E. Viterbo, “Low-complexity iterative detection for orthogonal time frequency space modulation,” in *Proc. IEEE WCNC,* Barcelona, April 2018.
9. P. Raviteja, K. T. Phan, Y. Hong, and E. Viterbo, “Interference cancellation and iterative detection for orthogonal time frequency space modulation,” *IEEE Trans. Wireless Commun.*, vol. 17, no. 10, pp. 6501-6515, Oct. 2018.
10. P. Raviteja, K. T. Phan, Y. Hong, and E. Viterbo, “Embedded delay-Doppler channel estimation for orthogonal time frequency space modulation,” in Proc. IEEE VTC2018-fall, Chicago, USA, August 2018.
11. P. Raviteja, K. T. Phan, and Y. Hong, “Embedded pilot-aided channel estimation for OTFS in delay-Doppler channels,” accepted in *IEEE Transactions on Vehicular Technology*.
12. P. Raviteja, Y. Hong, E. Viterbo, and E. Biglieri, “Practical pulse-shaping waveforms for reduced-cyclic-prefix OTFS,” *IEEE Trans. Veh. Technol.*, vol. 68, no. 1, pp. 957-961, Jan. 2019.
13. P. Raviteja, Y. Hong, and E. Viterbo, “OTFS performance on static multipath channels,” *IEEE Wireless Commun. Lett.*, Jan. 2019, doi: 10.1109/LWC.2018.2890643.
14. P. Raviteja, K.T. Phan, Y. Hong, and E. Viterbo, “Orthogonal time frequency space (OTFS) modulation based radar system,” accepted in *Radar Conference*, Boston, USA, April 2019.

References III

15. Li Li, H. Wei, Y. Huang, Y. Yao, W. Ling, G. Chen, P. Li, and Y. Cai, "A simple two-stage equalizer with simplified orthogonal time frequency space modulation over rapidly time-varying channels," available online: https://arxiv.org/abs/1709.02505.
16. T. Zemen, M. Hofer, and D. Loeschenbrand, "Low-complexity equalization for orthogonal time and frequency signaling (OTFS)," available online: https://arxiv.org/pdf/1710.09916.pdf.
17. T. Zemen, M. Hofer, D. Loeschenbrand, and C. Pacher, "Iterative detection for orthogonal precoding in doubly selective channels," available online: https://arxiv.org/pdf/1710.09912.pdf.
18. K. R. Murali and A. Chockalingam, "On OTFS modulation for high-Doppler fading channels," in *Proc. ITA'2018,* San Diego, Feb. 2018.
19. M. K. Ramachandran and A. Chockalingam, "MIMO-OTFS in high-Doppler fading channels: Signal detection and channel estimation," available online: https://arxiv.org/abs/1805.02209.
20. A. Farhang, A. RezazadehReyhani, L. E. Doyle, and B. Farhang-Boroujeny, "Low complexity modem structure for OFDM-based orthogonal time frequency space modulation," in *IEEE Wireless Communications Letters,* vol. 7, no. 3, pp. 344-347, June 2018.
21. A. RezazadehReyhani, A. Farhang, M. Ji, R. R. Chen, and B. Farhang-Boroujeny, "Analysis of discrete-time MIMO OFDM-based orthogonal time frequency space modulation," in *Proc. 2018 IEEE International Conference on Communications (ICC),* Kansas City, MO, USA, pp. 1-6, 2018.

Thank you!!